# INELASTIC EARTHQUAKE RESPONSE OF TALL R.C. BRIDGE PIERS WITH EMPHASIS ON ULTIMATE STATES

by

H. Goto(I), T. Kasai(II), and N. Imanishi(III)

## SUMMARY

Ultimate states of tall reinforced-concrete bridge piers subjected to strong earthquake motions are analyzed. Inelastic earthquake response is obtained for tall R.C. piers with variable sections. Discussion is made on the displacement, acceleration, bending moment, and curvature distribution. Emphasis is made on the excessive curvature developed in pier sections where rigidity changes discontinuously.

## DYNAMIC MODEL AND INPUT EARTHQUAKE MOTION

The dynamic model used in the response analysis is shown in Fig.1. It consists of an n-degree-of-freedom lumped mass system representing the pier and a rigid caisson with two degrees of freedom. Pier sections are assumed to have stiffness-degrading tri-linear hysteretic flexural rigidities proposed by Takeda, Sozen and Nielsen (Ref.1). A pier with 60m height shown in Fig.2 is used for a prototype, for which the dynamic model has been built to have five lumped masses. Hysteresis control is made for twenty five subelements defined by subdividing each pier element between lumped masses into five (Ref.2). The effect of foundation subsoil is represented by horizontal and rotational bilinear hysteretic springs $k_h$ and $k_r$. Their spring constants in the elastic region have been determined for A (hard), B (medium), and C (soft) soil conditions. The stiffness effect of the superstructure is represented by the spring $k_s$ connected to the pier top, and its mass effect is considered by attaching a part of its total mass to the top lumped mass.

Typical recorded accelerograms have been used for input earthquake motions, with adjusted peak accelerations of 200, 400, 600, 800, and 1000gals. All results presented in this papaer have been obtained for the NS component of the Kushiro, Japan, June 17, 1973 accelerogram, whose original peak acceleration was 187gals.

## RESULT OF RESPONSE ANALYSIS

Fig.3 shows the acceleration response at the first, third, and fifth nodes and on the caisson for the peak input acceleration of 400gals and for the subsoil A. The response of the first node is dominated by the fundamental mode of vibration with a period of 1.13sec, whereas the response of the other parts is dominated by the second mode with a period of 0.23sec.

---

(I) Professor, School of Civil Engineering, Kyoto University, Kyoto, Japan.
(II) Sumitomo Metal Industries, Osaka, Japan.
(III) Nippon Steel Corporation, Tokyo, Japan.

Fig.4 shows the variation of nondimensional flexural rigidities with time, demonstrating stiffness degradation in each subelement. It is observed that the concrete cracks throughout the pier around the time of 5sec. Yielding of reincorcement takes place at about 10sec, which causes excessive reduction of rigidity.

Fig.5 shows the distribution of the maximum displacement along the pier for various peak input accelerations. It is clear that the displacement is dominated by the fundamental mode. Fig.6 is a plot of the maximum displacement at the first node of the pier and that on the caisson. The data marked with x correspond to the cases where the subsoil failed. For the subsoils of type A and B, the displacement of the pier increases in proportion to the peak input acceleration, whereas in the case of the subsoil C, the displacements of the pier and the caisson both grow very large due to the failure of the subsoil.

Fig.7 shows the distribution of the maximum acceleration response for the case of subsoil A. The value of $K_0$=0.332 in this figure is the dsign seismic coefficient for the prototype pier, which was determined on the basis of a basic seismic coefficient of 0.2 modified with consideration of dynamic effects. Fig.8 shows the distribution of the maximum bending moment relative to the cracking moment $M_c$, yield moment $M_y$, and the static ultimate moment $M_u$. The bending moment obtained from a static analysis using the design seismic coefficient $K_0$ is also shown in the figure. Observe that the static value agrees well with the corresponding result of response analysis for the peak input acceleration of 200gals in spite of the result in Fig.7 where the acceleration response of the pier is considerably larger than $K_0$. Fig.9 shows the relation between the maximum bending moment at the base of the pier and the peak input acceleration.

Fig.10 shows the distribution of the maximum curvature developed in the pier with reference to the ductility factor $\mu$. Observe that initial yielding takes place in sections immediately above discontinuities of section rigidity. With increasing peak input acceleration, the curvatures in these discrete sections grow excessively. Such a concentration of deformation is particularly pronounced in the upper part of the pier where the moment grade is large. It may be noted, for example, that most part of the element between the nodes 2 and 3 is within the elastic range, whereas the bottom section of the element undergoes an excessively large curvature. In contrast, lower elements sustain inelastic deformations distributed more uniformly along the pier. It will be a subject for future studies whether of these two types of inelastic deformation should be aimed at in design. It may be pointed at this time that the composition of section rigidities along the pier axis should be determined considering these behaviors in the ultimate state.

## REFERENCES


(1) Takeda, T., Sozedn, M. A., and Nielsen, N. N., "Reinforced Concrete Response to Simulated Earthquakes," Journal of the Structural Division, ASCE, Vol.96, No.ST12, Dec. 1970, pp.2557-2573.

(2) Omote, Y., and Takeda, T., "Non-Linear Earthquake Response Study on the Reinforced Concrete Chimney," Trasactions of the Architectural Institute of Japan, No.215, Jan. 1974, pp.21-29, (in Japanese).

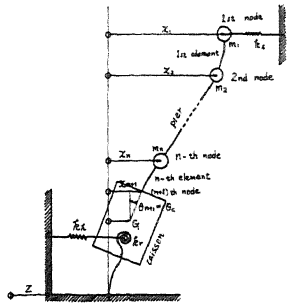


Fig.1 Dynamic Model of Pier-Caisson System.

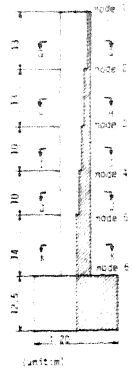

Fig.2 Prototype Tall R.C. Pier Used in This Study

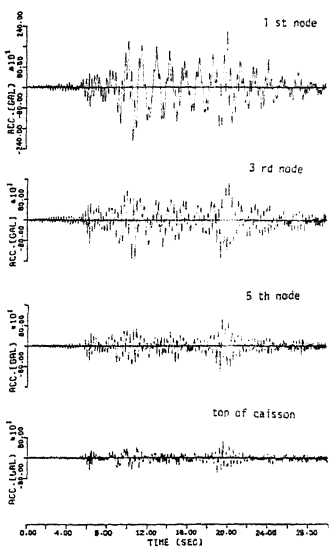


Fig.3 Absolute Acceleration Response (subsoil A, 400 gals input)

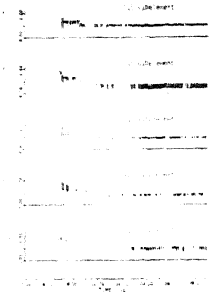

Fig.4 Degradation of Flexural Rigidity (subsoil C, 600 gals)

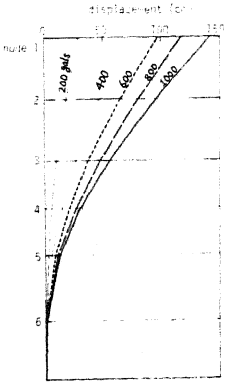


Fig.5 Peak Relative Displacement Response

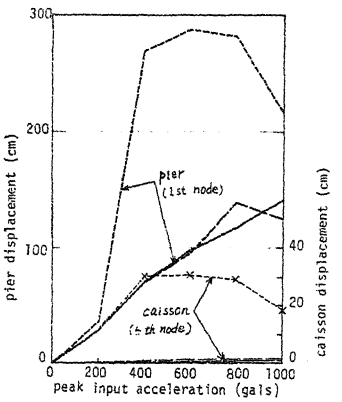


**Fig.**6 Peak Relative Displacement Response

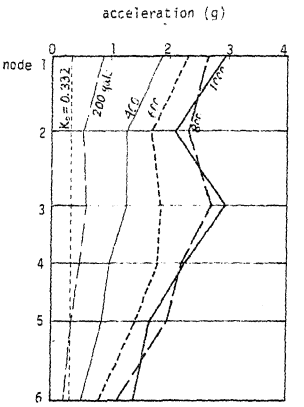


Fig.7 Peak Absolute Acceleration Response (subsoil A)

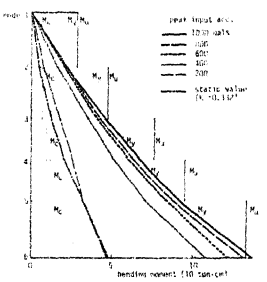

**Fig.**8 Bending Moment Distribution (subsoil A)

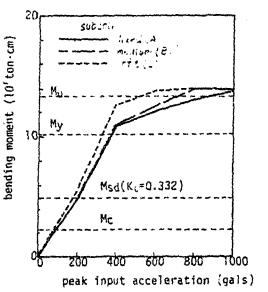


Fig.9 Maximum Bending Moment at Base of Pier

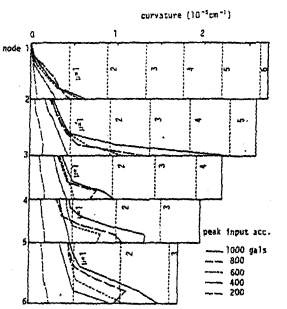


Fig.10 Curvature Distribution (subsoil A)